Antenna Placement and Power Allocation Optimization in MIMO Detection

MOJTABA RADMARD
MOHAMMAD MAHDI CHITGARHA, Student Member, IEEE
MOHAMMAD NAZARI MAJD, Student Member, IEEE
MOHAMMAD MAHDI NAYEBI, Senior Member, IEEE
Sharif University of Technology
Iran

It is a well known fact that using multiple antennas at transmit and receive sides improves the detection performance. However, in such multiple-input multiple-output (MIMO) configuration, proper positioning of transmitters and receivers is a big challenge that can have significant influence on the performance of the overall system. In addition, determining the power of each transmitter under a total power constraint is a problem that should be solved in order to enhance the performance and coverage of such a system. In this paper, we design the Neyman-Pearson detector under the Rayleigh scatter model and use it to introduce a criterion for the antenna placement at both transmit and receive sides. We then show that by using a waterfilling-type algorithm at the detector's output, optimum transmitter powers can be determined accordingly.

Manuscript received December 4, 2012; revised April 28, 2013, July 12, 2013; released for publication September 5, 2013.

DOI. No. 10.1109/TAES.2014.120776.

Refereeing of this contribution was handled by S. Watts.

Authors' address: Department of Electrical Engineering, Sharif University of Technology, Tehran, Iran. E-mail: (mojradmard@gmail.com).

I. INTRODUCTION

Recently, there has been significant interest towards use of multiple-input multiple-output (MIMO) in detection and localization. Generally, MIMO radars can be divided into two main categories: systems based on use of widely separated antennas and systems that use collocated antennas [1, 2].

In the case of widely separated antennas, multiple transmitters and multiple receivers that are widely separated are used in order to detect the objects of interest. The difference of this approach with multistatic systems lies in their jointly processing nature. As shown in [1], the concepts of spatial diversity and multiplexing gain emerge in this context in a dual manner to the MIMO communication. The main point is that, by looking at an object from different angles, the probability of missed detection decreases, a concept known as spatial diversity in MIMO communication. In [3, 4], it is shown that such diversity gain is available not only in the signal processing part but also in the data processing part. On the other hand, in the case of collocated antennas, such configuration is similar to phased array schemes, whereas, here the signals emitted by each antenna can be totally uncorrelated with each other.

The studies have shown that we can have enhanced detection performance (diversity gain) [5, 6] and high resolution object localization (spatial multiplexing gain) [7] with a widely separated antennas scheme.

The studies show that antennas' positions can affect the performance of the MIMO radar but little has been done on proper placement of such antennas. In [8], GDOP (geometric dilution of precision) is introduced as a metric that expresses the effect of the positions of the transmitting and receiving elements on the relationship between the time delay estimation errors and the localization errors. There, plots of GDOP are served as a tool for identifying the relation between antennas' positions and the obtainable accuracy. Finally, through a number of examples, it is shown that a symmetrical deployment of sensors around the object to be localized, yields the lowest GDOP values. Therefore, [8] does not introduce a procedure to position the antennas, but provides a tool to study the performance from an accuracy point of view. In addition, GDOP can be viewed as a metric for localization accuracy. Similarly, in [9, 10], plots of GDOP are used to provide an indication of localization accuracy over the two-dimensional space.

In [11], the Cramer-Rao bound (CRB) is derived for velocity estimation and is used to study the optimized system/configuration design based on CRB. In this case, the problem of antenna positioning is not addressed, but a tool is introduced to see the effect of antennas' positions on the velocity estimation of an object placed at a specific position.

It should be noted that in this paper, after designing a MIMIO detector, we introduce a criterion based on the detection performance, and not just on the estimation bound or the localization accuracy.

In [12–14], similar procedures are developed for placing the receive antennas in a MIMO passive coherent location (PCL) scheme, in which the noncooperative transmitters' positions and powers are not under control. In that scenario, the multiplication of the probabilities of missed detection of each receiver from each transmitter is used as a criterion. In addition, the signal model in the PCL is different from what we are considering here.

In [15], a scheme is proposed to adjust the power weights at the transmit antennas proportionally by taking into account the correlation and line-of-sight information present at the transmitters. Antennas that are correlated or perceive low line-of-sight reflectivity are allocated less power so that the total available energy is spread across diversity branches and strong reflectors, accordingly. It is shown that this work will alleviate the performance of MIMO systems in the existence of correlation and Ricean scattering models. However, in this manuscript, we consider the Rayleigh scatter model for the objects (Swerling model) and do the power allocation without the assumption of having such information at the transmit side.

In [16–18], the energy allocation is adopted to improve the detection of a target, for which the RCS and location have been estimated before. But, in this paper the target behaves as a Rayleigh scatterer and the power allocation is done in order to improve the performance over the whole region of interest. In addition, in [19], the proposed resource allocation scheme to maximize the minimum probability of detection in the surveillance area assumes that the target's RCS has a zero-mean complex Gaussian distribution.

In [20], two resource allocation schemes for multiple detection systems are proposed. The first approach fully utilizes all available infrastructure in the localization process, i.e., all transmit and receive systems, while minimizing the total transmit energy. The power allocation among the transmit antennas is optimized such that a predefined estimation mean-square error (MSE) objective is met, while keeping the transmitted power at each station within an acceptable range. The second scheme minimizes the number of transmit and receive antennas employed in the estimation process by effectively choosing a subset of antennas such that the required MSE performance threshold is attained. Here, similarly, only the estimation is considered, while we need to detect the object first.

II. TRANSMITTERS' POSITIONING

The power of the transmitted signal from the transmitter at $\tilde{X}$ seen by an object located at the position $\tilde{Z}$ can be computed as below

$$P_r = \frac{P_t \sigma_t^2}{4\pi R^2 L_c} \tag{1}$$

where P_t, R, σ_t^2, and L_c are the transmitter power, distance between transmitter and object, radar cross section (RCS) of object, and scattering loss, respectively.

We use this power as the criterion for placing the transmitters. The procedure is as follows.

First, we intend to find the best position of the first transmitter. For a transmitter located at a specific $\tilde{X}$ in the region of interest, we compute the average power of (1) by changing the position of the object ($\tilde{Z}$) over the whole region of interest. The resulting average power will be an indicator of how much $\tilde{X}$ is good to place the transmitter. After changing $\tilde{X}$ all over the region of interest (the radar's surveillance region) and computing the average power for each one, the position resulting in the highest average power is chosen as the best position for placing the first transmit antenna ($\hat{X}_1$).

In order to find the best position of the second transmitter, we repeat the mentioned procedure, however, with a little modification. This time we use the reciprocal of the first transmitter's power (which is already positioned at $\hat{X}_1$) at each $\tilde{Z}$ as a weighting coefficient, before taking the average. We do this so that the second transmitter compensates the first one at locations where the first one's power is low.

Finding the next transmitters' positions are similar to the second one. But it should be noted that for each one, the weighting coefficient is the reciprocal of the sum of the previously positioned transmitters' powers.

III. RECEIVERS' POSITIONING

A. Neyman-Pearson Detector

First, the goal is to find a criterion, based on which, we can choose the positions of the receivers.

Here, we design the Neyman-Pearson detector while having multiple antennas at transmit and receive sides. We assume the orthogonality of the transmitted signals, i.e.,

$$\int_{-\infty}^{\infty} s_k(t) s_k'^{*}(t+\tau)\, dt = \begin{cases} 1 & \text{if } k = k', \tau = 0 \\ 0 & \text{otherwise} \end{cases} \tag{2}$$

Let the coordinate vectors of the transmitters' positions and the receivers' positions be denoted by $TX_m (1 \le m \le N_i)$ and $RX_n (1 \le n \le N_r)$, respectively. Now, consider the hypothesis in which we assume an object exists in the specific bistatic range corresponding to the position $\tilde{Y}$. The bistatic range of the echo from the i'th transmitter at the r'th receiver will be

$$r_{it} + r_{tr} \tag{3}$$

where r_{it} and r_{tr} represent the (i'th TX-object) and (object-r'th RX) distance, respectively. We use Neyman-Pearson detector [21] since priori probabilities are unknown. Therefore, the likelihood ratio L($\mathbf{y}$) (defined in (13)) is compared with threshold value η, which is determined according to the false alarm probability. Therefore, in the $\mathcal{H}_0$ hypothesis, i.e., in the absence of the object to be localized, the received signal is pure noise. However, in the $\mathcal{H}_1$ hypothesis, i.e., in the presence of an object, the received signal is the sum of the echo signal and pure noise. In the following, the signal model that is

based on such hypotheses is given for each receiver.

$$\begin{aligned}\mathcal{H}_0 &: \mathbf{y}_r = \mathbf{n} && r = 1, \ldots, N_r \\ \mathcal{H}_1 &: \mathbf{y}_r = \mathbf{n} + \Sigma_{i=1}^{N_i} \alpha_{ri} \mathbf{s}_i(t - \tau_{ri}) && r = 1, \ldots, N_r\end{aligned} \tag{4}$$

where $\mathbf{y}_r$, $\mathbf{s}_i$, and $\mathbf{n}$ are the received signal, i'th transmitter signal, and additive white Gaussian noise vectors at the r'th receiver, respectively. Also τ_{ri} is the bistatic range delay (i'th TX-object-r'th RX) and α_{ri} is the amplitude of the received signal. We assume the Swerling I model for the RCS of the object:

$$f_{\sigma_t}(x) = \frac{x}{\sigma_0^2} e^{-\frac{x^2}{2\sigma_0^2}} \tag{5}$$

where σ_0^2 is the average RCS of the object. Therefore, according to the free space propagation loss equation, we can write

$$\alpha_{ri} = \frac{\sigma_t}{r_{1i} r_{2i}} \sqrt{\frac{P_t G_t G_r I_p \lambda^2}{(4\pi)^3 L_c L_r}} \tag{6}$$

In the above equation, P_t is the transmitted power, G_t and G_r are the transmitting and receiving antenna gains, respectively, I_p is the processing gain at the receiver, λ is wavelength, L_c is the scattering loss, and L_r is the receiver loss. From (5), (6)

$$f_{\alpha_{ri}}(x) = \frac{x}{\sigma_{ri}^2} e^{-\frac{x^2}{2\sigma_{ri}^2}} \tag{7}$$

where

$$\sigma_{ri}^2 = \frac{P_t G_t G_r I_p \sigma_0^2 \lambda^2}{(4\pi)^3 r_{1i}^2 r_{2i}^2 L_c L_r} \tag{8}$$

As the antennas are widely separated, we can assume that the different σ_{ri}s are independent [1]. If we consider Gaussian distribution function for noise, by using hypothesis signal models,

$$f_{\mathbf{Y}_r}(\mathbf{y}_r|\mathcal{H}_0) \sim \mathcal{N}(0, \sigma^2 I)$$

$$f_{\mathbf{Y}_r}(\mathbf{y}_r|\mathcal{H}_1, \alpha_{ri}) \sim \mathcal{N}(\mathbf{s}_{0r}, \sigma^2 I) \tag{9}$$

In the above equation σ^2 is the noise variance, $\mathbf{y}_r$ is the r'th receiver signal vector, and

$$\mathbf{s}_{0r} \triangleq \Sigma_{i=1}^{N_i} \alpha_{ri} \mathbf{s}_i(t - \tau_{ri}) \tag{10}$$

We define

$$\mathbf{s}_0 \triangleq [\mathbf{s}_{01}\ \mathbf{s}_{02}\ \ldots\ \mathbf{s}_{0N_r}]^T \tag{11}$$

and,

$$\mathbf{y} \triangleq [\mathbf{y}_1\ \mathbf{y}_2\ \ldots\ \mathbf{y}_{N_r}]^T \tag{12}$$

where $\mathbf{y}$ consists of the received signal vectors of all receivers.

We can write the likelihood ratio for the Neyman-Pearson detector as the following.

$$L(\mathbf{y}) = \frac{f_{\mathbf{Y}}(\mathbf{y}|\mathcal{H}_1)}{f_{\mathbf{Y}}(\mathbf{y}|\mathcal{H}_0)} \tag{13}$$

In this way, we can set the threshold from the desired probability of false alarm.

$$f_{\mathbf{Y}}(\mathbf{y}|\mathcal{H}_0) = \frac{1}{(2\pi\sigma^2)^{N/2}} \Pi_{r=1}^{N_r} \{e^{-\frac{\|\mathbf{y}_r\|^2}{2\sigma^2}}\} \tag{14}$$

where N is the length of the received vector. From (9) we have

$$\begin{aligned} f_{\mathbf{Y}}(\mathbf{y}|\mathcal{H}_1) &= \int_0^\infty \ldots \int_0^\infty f_{\mathbf{Y}}(\mathbf{y}|\mathcal{H}_1, \alpha_{ri}) \Pi_{i=1}^{N_i} \Pi_{r=1}^{N_r} f_{\alpha_{ri}}(\alpha_{ri}) d\alpha_{ri} \\ &= \int_0^\infty \ldots \int_0^\infty \frac{1}{(2\pi\sigma^2)^{N/2}} e^{-\frac{\|\mathbf{y}-\mathbf{s}_0\|^2}{2\sigma^2}} \Pi_{i=1}^{N_i} \Pi_{r=1}^{N_r} f_{\alpha_{ri}}(\alpha_{ri}) d\alpha_{ri} \\ &= \int_0^\infty \ldots \int_0^\infty \frac{1}{(2\pi\sigma^2)^{N/2}} e^{-\frac{\|\mathbf{y}\|^2 - 2\mathbf{y}^T\mathbf{s}_0 + \|\mathbf{s}_0\|^2}{2\sigma^2}} \\ &\quad \times \Pi_{i=1}^{N_i} \Pi_{r=1}^{N_r} f_{\alpha_{ri}}(\alpha_{ri}) d\alpha_{ri} \end{aligned} \tag{15}$$

As mentioned earlier, the transmitted signals are orthogonal, so that

$$\mathbf{s}_i^T(t - \tau_{ri}) \mathbf{s}_j(t - \tau_{rj}) = \delta_{ij} \tag{16}$$

Therefore,

$$\begin{aligned} \|\mathbf{s}_0\|^2 &= \mathbf{s}_0^T \mathbf{s}_0 = \Sigma_{r=1}^{N_r} \mathbf{s}_{0r}^T \mathbf{s}_{0r} \\ &= \Sigma_{r=1}^{N_r} \Sigma_{i=1}^{N_i} \Sigma_{j=1}^{N_j} \alpha_{ri} \mathbf{s}_i^T(t - \tau_{ri}) \alpha_{rj} \mathbf{s}_j(t - \tau_{rj}) \\ &= \Sigma_{r=1}^{N_r} \Sigma_{i=1}^{N_i} \alpha_{ri}^2 \end{aligned} \tag{17}$$

$$\|\mathbf{y}\|^2 = \Sigma_{r=1}^{N_r} \|\mathbf{y}_r\|^2 = \frac{1}{N_i} \Sigma_{i=1}^{N_i} \Sigma_{r=1}^{N_r} \|\mathbf{y}_r\|^2 \tag{18}$$

$$\begin{aligned} \mathbf{y}^T \mathbf{s}_0 &= \Sigma_{r=1}^{N_r} \mathbf{y}_r^T \Sigma_{i=1}^{N_i} \alpha_{ri} \mathbf{s}_i(t - \tau_{ri}) \\ &= \Sigma_{r=1}^{N_r} \Sigma_{i=1}^{N_i} \alpha_{ri} \mathbf{y}_r^T \mathbf{s}_i(t - \tau_{ri}) \end{aligned} \tag{19}$$

and

$$\begin{aligned} f_{\mathbf{Y}}(\mathbf{y}|\mathcal{H}_1) &= \int_0^\infty \ldots \int_0^\infty \frac{1}{(2\pi\sigma^2)^{N/2}} \\ &\quad \times e^{-\frac{\Sigma_{i=1}^{N_i} \Sigma_{r=1}^{N_r} \left(\frac{1}{N_i} \|\mathbf{y}_r\|^2 - 2\alpha_{ri} \mathbf{y}_r^T \mathbf{s}_i(t-\tau_{ri}) + \alpha_{ri}^2 \right)}{2\sigma^2}} \\ &\quad \times \Pi_{i=1}^{N_i} \Pi_{r=1}^{N_r} f_{\alpha_{ri}}(\alpha_{ri}) d\alpha_{ri} \\ &= \frac{1}{(2\pi\sigma^2)^{N/2}} \Pi_{i=1}^{N_i} \Pi_{r=1}^{N_r} \\ &\quad \int_0^\infty e^{-\frac{\frac{1}{N_i}\|\mathbf{y}_r\|^2 - 2\alpha_{ri}\mathbf{y}_r^T\mathbf{s}_i(t-\tau_{ri}) + \alpha_{ri}^2}{2\sigma^2}} f_{\alpha_{ri}}(\alpha_{ri}) d\alpha_{ri} \\ &= \frac{1}{(2\pi\sigma^2)^{N/2}} \Pi_{i=1}^{N_i} \Pi_{r=1}^{N_r} I_{ri} \end{aligned} \tag{20}$$

where

$$I_{ri} = \int_0^\infty e^{-\frac{\frac{1}{N_i}\|\mathbf{y}_r\|^2 - 2\alpha_{ri}\mathbf{y}_r^T\mathbf{s}_i(t-\tau_{ri}) + \alpha_{ri}^2}{2\sigma^2}} f_{\alpha_{ri}}(\alpha_{ri}) d\alpha_{ri} \tag{21}$$

Substituting from (7), we have

$$I_{ri} = \int_0^\infty e^{-\frac{\frac{1}{N_i}\|\mathbf{y}_r\|^2 - 2x\mathbf{y}_r^T\mathbf{s}_i(t-\tau_{ri})+x^2}{2\sigma^2}} \frac{x}{\sigma_{ri}^2} e^{-\frac{x^2}{2\sigma_{ri}^2}} dx$$
$$= e^{-\frac{\|\mathbf{y}_r\|^2}{2N_i\sigma^2}} \int_0^\infty \frac{x}{\sigma_{ri}^2} e^{-\frac{x^2 - 2x\mathbf{y}_r^T\mathbf{s}_i(t-\tau_{ri})}{2\sigma^2} - \frac{x^2}{2\sigma_{ri}^2}} dx$$
$$= \frac{e^{-\frac{\|\mathbf{y}_r\|^2}{2N_i\sigma^2}}}{\sigma_{ri}^2} \int_0^\infty x e^{-\frac{1}{2}(\frac{1}{\sigma^2}+\frac{1}{\sigma_{ri}^2})x^2 + \frac{x}{\sigma^2}\mathbf{y}_r^T\mathbf{s}_i(t-\tau_{ri})} dx$$
$$= \frac{e^{-\frac{\|\mathbf{y}_r\|^2}{2N_i\sigma^2}}}{\sigma_{ri}^2} \int_0^\infty x e^{-a_{1ri}^2x^2 + a_{2ri}x} dx \quad (22)$$

where

$$a_{1ri}^2 = \frac{1}{2}(\frac{1}{\sigma^2} + \frac{1}{\sigma_{ri}^2})$$
$$a_{2ri} = \frac{1}{\sigma^2}\mathbf{y}_r^T\mathbf{s}_i(t-\tau_{ri}) \quad (23)$$

so,

$$I_{ri} = \frac{e^{-\frac{\|\mathbf{y}_r\|^2}{2N_i\sigma^2}}}{\sigma_{ri}^2} \int_0^\infty x e^{-(a_{1ri}x - \frac{a_{2ri}}{2a_{1ri}})^2} e^{\frac{a_{2ri}^2}{4a_{1ri}^2}} dx \quad (24)$$

If we define

$$u = a_{1ri}x - \frac{a_{2ri}}{2a_{1ri}} \quad (25)$$

then

$$I_{ri} = \frac{e^{\frac{a_{2ri}^2}{4a_{1ri}^2} - \frac{\|\mathbf{y}_r\|^2}{2N_i\sigma^2}}}{\sigma_{ri}^2} (\int_{-\frac{a_{2ri}}{2a_{1ri}}}^\infty \frac{1}{a_{1ri}^2} u e^{-u^2} du$$
$$+ \int_{-\frac{a_{2ri}}{2a_{1ri}}}^\infty \frac{a_{2ri}}{2a_{1ri}^3} e^{-u^2} du)$$
$$= \frac{e^{-\frac{\|\mathbf{y}_r\|^2}{2N_i\sigma^2}}}{2a_{1ri}^2\sigma_{ri}^2}(1 + \frac{a_{2ri}}{a_{1ri}}\sqrt{\pi}e^{\frac{a_{2ri}^2}{4a_{1ri}^2}} Q(-\frac{a_{2ri}}{\sqrt{2}a_{1ri}}))$$
$$= \frac{e^{-\frac{\|\mathbf{y}_r\|^2}{2N_i\sigma^2}}}{1+\frac{\sigma_{ri}^2}{\sigma^2}}(1 + \frac{a_{2ri}}{a_{1ri}}\sqrt{\pi}e^{\frac{a_{2ri}^2}{4a_{1ri}^2}} Q(-\frac{a_{2ri}}{\sqrt{2}a_{1ri}})) \quad (26)$$

Substituting this result in (20),

$$f_{\mathbf{Y}}(\mathbf{y}|\mathcal{H}_1) = \frac{1}{(2\pi\sigma^2)^{N/2}} \Pi_{i=1}^{N_i}\Pi_{r=1}^{N_r}$$
$$\{\frac{e^{-\frac{\|\mathbf{y}_r\|^2}{2N_i\sigma^2}}}{1+\frac{\sigma_{ri}^2}{\sigma^2}}(1 + \frac{a_{2ri}}{a_{1ri}}\sqrt{\pi}e^{\frac{a_{2ri}^2}{4a_{1ri}^2}} Q(-\frac{a_{2ri}}{\sqrt{2}a_{1ri}}))\} \quad (27)$$

Substituting (14), (27) in (13) yields

$$L(\mathbf{y}) = \frac{f_{\mathbf{Y}}(\mathbf{y}|\mathcal{H}_1)}{f_{\mathbf{Y}}(\mathbf{y}|\mathcal{H}_0)}$$
$$= \Pi_{i=1}^{N_i}\Pi_{r=1}^{N_r}\{\frac{1}{1+\frac{\sigma_{ri}^2}{\sigma^2}}(1+\frac{a_{2ri}}{a_{1ri}}\sqrt{\pi}e^{\frac{a_{2ri}^2}{4a_{1ri}^2}} Q(-\frac{a_{2ri}}{\sqrt{2}a_{1ri}}))\} \quad (28)$$

If $L(\mathbf{y})$ is greater than the threshold, $\mathcal{H}_1$ is chosen, otherwise $\mathcal{H}_0$ is chosen.

$$L(\mathbf{y}) \gtrless \eta_1 \quad (29)$$

Then,

$$\Pi_{i=1}^{N_i}\Pi_{r=1}^{N_r}\{\frac{1}{1+\frac{\sigma_{ri}^2}{\sigma^2}}(1 + \frac{a_{2ri}}{a_{1ri}}\sqrt{\pi}e^{\frac{a_{2ri}^2}{4a_{1ri}^2}} Q(-\frac{a_{2ri}}{\sqrt{2}a_{1ri}}))\} \gtrless \eta_1 \quad (30)$$

With removing the constant term,

$$\Pi_{i=1}^{N_i}\Pi_{r=1}^{N_r}\{(1 + \frac{a_{2ri}}{a_{1ri}}\sqrt{\pi}e^{\frac{a_{2ri}^2}{4a_{1ri}^2}} Q(-\frac{a_{2ri}}{\sqrt{2}a_{1ri}}))\} \gtrless \eta_2 \quad (31)$$

As $L(\mathbf{y})$ is always positive and logarithmic function is monotonic, $\mathrm{Log}(L(\mathbf{y}))$ can be compared with new threshold. Thus,

$$\Sigma_{i=1}^{N_i}\Sigma_{r=1}^{N_r}\{\mathrm{Log}(1 + \frac{a_{2ri}}{a_{1ri}}\sqrt{\pi}e^{\frac{a_{2ri}^2}{4a_{1ri}^2}} Q(-\frac{a_{2ri}}{\sqrt{2}a_{1ri}}))\} \gtrless \eta \quad (32)$$

This detector is optimal for the above MIMO problem, so we define the following statistic

$$T \triangleq \Sigma_{i=1}^{N_i}\Sigma_{r=1}^{N_r}\{\mathrm{Log}(1 + \frac{a_{2ri}}{a_{1ri}}\sqrt{\pi}e^{\frac{a_{2ri}^2}{4a_{1ri}^2}} Q(-\frac{a_{2ri}}{\sqrt{2}a_{1ri}}))\} \quad (33)$$

As this statistic is always positive, the following expression can be an indicator of the detector's output signal-to-noise ratio (SNR). The reduction is a consequence of the logarithmic property.

$$\mathrm{SNR} = E\{T|\mathcal{H}_1\} - E\{T|\mathcal{H}_0\} \quad (34)$$

In Appendix B, it is shown that $E\{T|\mathcal{H}_1\}$ and $E\{T|\mathcal{H}_0\}$ are monotonically increasing functions of $\frac{a_{2ri}}{a_{1ri}}|\mathcal{H}_1$ and $\frac{a_{2ri}}{a_{1ri}}|\mathcal{H}_0$, respectively. Consequently, an increase in the difference of $\frac{a_{2ri}}{a_{1ri}}|\mathcal{H}_1$, $\frac{a_{2ri}}{a_{1ri}}|\mathcal{H}_0$ will lead to an increase in the difference of $E\{T|\mathcal{H}_1\}$, $E\{T|\mathcal{H}_0\}$ which means an increase in SNR. It can be seen from the following equation that by increasing an object's RCS, decreasing noise power, increasing received signal energy (i.e., decreasing the bistatic range, increasing transmit power, antenna and other gains) and better signal matching, detection is better and lower missed detection is achieved as expected.

$$\frac{a_{2ri}}{a_{1ri}}|\mathcal{H}_1 - \frac{a_{2ri}}{a_{1ri}}|\mathcal{H}_0$$
$$= \frac{\sqrt{2}}{\sigma\sqrt{1+\frac{\sigma^2}{\sigma_{ri}^2}}}(((n + \Sigma_{i=1}^{N_i}\alpha_{ri}s_i(t-\tau_{ri})) - n)^T s_i(t-\tau_{ri})) \quad (35)$$

Such approach is used as the criterion for receivers' positioning according to the procedure we introduce later. Due to complicated integral computations in finding expectations, a numerical approach is adopted.

B. SNR as a Criterion for Placing the Receive Antennas

Here, we use the detector's output SNR (34) as a criterion to find the proper positions for placing the

receivers. The procedure of placing the receive antennas is similar to the procedure of placing transmit antennas.

Each of the region's positions is a candidate for placing the first receive antenna at that point. Suppose we place the receiver at the point $\tilde{Y}$. So, for the position $\tilde{Y}$, we can compute output SNR of the detector. However, the value of SNR changes by changing the position of the object ($\tilde{Z}$). Therefore, we evaluate the average of the values of SNRs after changing the object's position ($\tilde{Z}$) in the whole region. Subsequently, this average SNR can be a criterion of how much $\tilde{Y}$ is good for placing the receiver. The position $\tilde{Y}$ resulting in the highest average SNR is chosen to place the first reciver.

To locate the next receivers, we repeat this procedure. However, before taking the average, we use the reciprocal of the SNR, gained from the previously located receivers, at each $\tilde{Z}$ as a weighting coefficient.

IV. POWER ALLOCATION

In the previous stage (antenna placement), for simplification, we have assumed all the transmitters have the same power. The next step of setting up our MIMO system is to define each transmitter's power in order to improve the performance. Here, the constraint is that overall power is constant.

A. Solution Approach

Now that the antennas' positions are determined, we need to introduce a criterion for each power allocation scheme when the object is at a specific location, e.g. $\tilde{Z}$. As we are dealing with $L(\mathbf{y})$ in the detection process, we claim that $E\{L(\mathbf{y}|\mathcal{H}_1)\}$ is a suitable criterion for our purpose, where $L(\mathbf{y})$ is defined in (28). However, $E\{L(\mathbf{y}|\mathcal{H}_0)\}$ is independent of the powers transmitted and is only a function of noise. Therefore, the power allocation scheme, which leads to higher $E\{L(\mathbf{y}|\mathcal{H}_1)\}$ has better detection performance. The details of computing $E\{L(\mathbf{y}|\mathcal{H}_1)\}$ as a closed form are described in the next section. We show that the proposed approach will lead to the well-known waterfilling technique. After computing the power levels of each transmitter for the object located at $\tilde{Z}$, we change $\tilde{Z}$ all over the region of interest and take the average of the resulting power levels to use as the final allocated power to the transmitters.

B. Obtaining the Power Allocation Criterion

In order to decrease the complexity of the detector, we assume it is working at high SNR. Consequently, we can assume

$$\frac{\sigma_{ri}}{\sigma} \gg 1 \tag{36}$$

Such assumption is not unusual by considering the processing gain. For example, if we assume the common parameters of Table I and the assumption that $r_{1i},\ r_{2i} < 30$ Km, then from (8) we have

$$\frac{\sigma_{ri}^2}{\sigma^2} = 85.3 = 19.3dB \tag{37}$$

TABLE I
Sample Parameters

P_t	30 kW
N_i	3
N_r	3
λ	3 cm
$R_r = G_t$	20 dB
F_n	7 dB
I_p	45 dB
$L_c = L_r$	0 dB
σ_0^2	$2\,m^2$
BW	6 MHz

By this assumption, we have

$$a_{1ri}^2 = \frac{1}{2\sigma^2} \tag{38}$$

$$a_{2_{ri}}|\mathcal{H}_1 = \frac{\mathbf{y}_r^T.\mathbf{s}(t-\tau_{ri})}{\sigma^2}|\mathcal{H}_1 \approx \frac{\alpha_{ri}}{\sigma^2} = \frac{\nu_{ri}\sqrt{P_i}}{\sigma^2} \tag{39}$$

where

$$\nu_{ri}^2 = \frac{\alpha_{ri}^2}{P_i} \tag{40}$$

Therefore, from (28) we have

$$\begin{aligned} L(\mathbf{y}) &\approx \Pi_{i=1}^{N_i}\Pi_{r=1}^{N_r} \\ &\{\frac{1}{1+\frac{\sigma_{ri}^2}{\sigma^2}}(1+\sqrt{2\pi}\sigma a_{2ri}e^{\frac{a_{2ri}^2}{4a_{1ri}^2}}(1-\frac{1}{\sqrt{2\pi}\sigma a_{2ri}}e^{-\frac{a_{2ri}^2}{4a_{1ri}^2}}))\} \\ &= \Pi_{i=1}^{N_i}\Pi_{r=1}^{N_r}\{\frac{1}{1+\frac{\sigma_{ri}^2}{\sigma^2}}\sqrt{2\pi}\sigma a_{2ri}e^{\frac{a_{2ri}^2}{2}\sigma^2}\} \end{aligned} \tag{41}$$

where we have used

$$Q(-x) \approx 1 - \frac{1}{\sqrt{2\pi}x}e^{-\frac{x^2}{2}},\ x \gg 1 \tag{42}$$

So,

$$\ln L(\mathbf{y}|\mathcal{H}_1) = \sum_{i=1}^{N_i}\sum_{r=1}^{N_r}\ln(\sqrt{\pi}x_{ri}e^{\frac{x_{ri}^2}{4}}) - \ln(1+\frac{\sigma_{ri}^2}{\sigma^2}) \tag{43}$$

where

$$x_{ri} = \frac{a_{2_{ri}}}{a_{1_{ri}}} = \frac{\frac{\nu_{ri}\sqrt{P_i}}{\sigma^2}}{\sqrt{\frac{1}{2\sigma^2}}} = \frac{\nu_{ri}\sqrt{2P_i}}{\sigma} \tag{44}$$

The constraint is that the sum of the transmitters' powers is constant, i.e.,

$$\sum_{i=1}^{N_i} P_i = P \tag{45}$$

In order to find the optimum power allocation between transmitters, we form the Lagrangian

$$\mathcal{L} = \sum_{i=1}^{N_i}\sum_{r=1}^{N_r} \ln(\sqrt{\pi} x_{ri} e^{\frac{x_{ri}^2}{4}}) - \ln(1+\frac{\nu_{ri}^2}{\sigma^2}P_i) - \mu\sum_{i=1}^{N_i} P_i \tag{46}$$

Consequently,

$$\frac{\partial \mathcal{L}}{\partial P_i} = \sum_{r=1}^{N_r}(\frac{z_{ri}}{x_{ri}} + \frac{x_{ri}}{2}z_{ri}) - \frac{\nu_{ri}^2}{\sigma^2+\nu_{ri}^2 P_i} - \mu = 0 \tag{47}$$

where

$$\begin{aligned} z_{ri} &= \frac{\partial x_{ri}}{\partial P_i} = \frac{\partial(\frac{a_{2_{ri}}}{a_{1_{ri}}})}{\partial P_i} = \frac{\frac{\partial a_{2_{ri}}}{\partial P_i}a_{1_{ri}} - \frac{\partial a_{1_{ri}}}{\partial P_i}a_{2_{ri}}}{a_{1_{ri}}^2} \\ \frac{\partial a_{2_{ri}}}{\partial P_i} &= \frac{\nu_{ri}}{2\sigma^2\sqrt{P_i}} \\ \frac{\partial a_{1_{ri}}}{\partial P_i} &= \frac{-\frac{1}{2\nu_{ri}^2 P_i^2}}{2\sqrt{\frac{1}{2}(\frac{1}{\sigma^2}+\frac{1}{\nu_{ri}P_i})}} \end{aligned} \tag{48}$$

and the parameter μ is varied such that the whole power becomes P from (48)

$$\begin{aligned} z_{ri} &= \frac{\frac{\nu_{ri}}{2\sigma^2\sqrt{P_i}}\sqrt{\frac{1}{2}(\frac{1}{\sigma^2}+\frac{1}{\nu_{ri}^2P_i})} + \frac{1}{4\nu_{ri}^2P_i^2\sqrt{\frac{1}{2}(\frac{1}{\sigma^2}+\frac{1}{\nu_{ri}^2P_i})}}\cdot\frac{\nu_{ri}\sqrt{P_i}}{\sigma^2}}{\frac{1}{2}(\frac{1}{\sigma^2}+\frac{1}{\nu_{ri}^2P_i})} \\ &= \frac{\frac{\nu_{ri}}{2\sigma^2\sqrt{P_i}}(\frac{1}{2}(\frac{1}{\sigma^2}+\frac{1}{\nu_{ri}^2P_i})) + \frac{\nu_{ri}\sqrt{P_i}}{4\sigma^2\nu_{ri}^2P_i^2}}{(\frac{1}{2}(\frac{1}{\sigma^2}+\frac{1}{\nu_{ri}^2P_i}))^{\frac{3}{2}}} \end{aligned} \tag{49}$$

Using the assumption of (36), the term $\frac{1}{\nu_{ri}^2P_i}$ can be neglected and z_{ri} is simplified as

$$\begin{aligned} z_{ri} &= \frac{\frac{\nu_{ri}}{2\sigma^2\sqrt{P_i}}\cdot\frac{1}{2\sigma^2} + \frac{1}{4\sigma^2\nu_{ri}P_i^{\frac{3}{2}}}}{\frac{1}{2\sigma^2}\sqrt{\frac{1}{2\sigma^2}}} \\ &= \frac{\nu_{ri}+\sigma^2\frac{1}{\nu_{ri}P_i}}{\sqrt{2\sigma^2}\sqrt{P_i}} = \frac{\nu_{ri}}{\sigma\sqrt{2P_i}} \end{aligned} \tag{50}$$

Substituting (44) and (50) into (47), yields

$$\sum_{r=1}^{N_r}(\frac{\nu_{ri}}{\sigma\sqrt{2P_i}}(\frac{\sigma}{\nu_{ri}\sqrt{2P_i}}+\frac{\nu_{ri}\sqrt{2P_i}}{2\sigma}) - \frac{\nu_{ri}^2}{\sigma^2+\nu_{ri}^2P_i}) - \mu = 0 \tag{51}$$

$$\sum_{r=1}^{N_r}(\frac{1}{2P_i} + \frac{\nu_{ri}^2}{2\sigma^2} - \frac{\nu_{ri}^2}{\sigma^2+\nu_{ri}^2P_i}) - \mu = 0 \tag{52}$$

Using the assumption of (36) again, the third term of (52) is simplified as below

$$\frac{\nu_{ri}^2}{\sigma^2+\nu_{ri}^2P_i} = \frac{\frac{1}{P_i}}{\frac{\sigma^2}{\nu_{ri}^2P_i}+1} \approx \frac{1}{P_i} \tag{53}$$

Thus,

$$-\frac{N_r}{2P_i} + \frac{\sum_{r=1}^{N_r}\nu_{ri}^2}{2\sigma^2} = \mu \tag{54}$$

$$P_i = (\frac{N_r}{2}\frac{1}{\frac{\sum_{r=1}^{N_r}\nu_{ri}^2}{2\sigma^2}-\mu})^+ = (\frac{N_r}{\sum_{r=1}^{N_r}(\frac{\nu_{ri}}{\sigma})^2 - 2\mu})^+ \tag{55}$$

where the notation $(P)^+$ denotes that if P is negative, it is set zero. Note that if X is a Rayleigh random variable with parameter $\sqrt{\frac{1}{\gamma}}$, X^2 has an exponential density with parameter $\frac{\gamma}{2}$. Here, σ_{ri} has Rayleigh density with parameter σ_t. So, $\frac{\nu_{ri}^2}{\sigma^2}\sigma_{ri}^2$ has exponential distribution with parameter $\mu_i = \frac{\sigma^2}{2\nu_{ri}^2\sigma_t^2}$. Thus, the first term of the denominator of (55) is the sum of N_r exponential variables with parameter $\frac{\sigma^2}{2\nu_{ri}^2\sigma_t^2}$. In Appendix A, the density of the summation of exponential variables with parameter μ is obtained as follows

$$f_S(s) = (\prod_{j=1}^{N_r}\mu_j)\sum_{j=1}^{N_r}\frac{e^{-\mu_j s}}{\prod_{k=1,k\neq j}^{N_r}(\mu_k-\mu_j)}, s>0 \tag{56}$$

where s is the summation variable:

$$s = \sum_{r=1}^{N_r}\frac{\nu_{ri}^2}{\sigma^2}\sigma_{ri}^2 \tag{57}$$

The above power is for a specific realization of the object's RCS (which was a Rayleigh random variable). For our purpose, we need to take the expected value of (55).

$$\begin{aligned} P_i &= (\int_0^\infty \frac{N_r}{s-2\mu}(\prod_{i=1}^{N_r}\mu_i)\sum_{j=1}^{N_r}\frac{e^{-\mu_j s}}{\prod_{k=1,k\neq j}^{N_r}(\mu_k-\mu_j)}ds)^+ \\ &= (N_r(\prod_{i=1}^{N_r}\mu_i)\int_0^\infty\sum_{j=1}^{N_r}\frac{1}{\prod_{k=1,k\neq j}^{N_r}(\mu_k-\mu_j)}\frac{e^{-\mu_j s}}{s-2\mu}ds)^+ \\ &= (N_r(\frac{\sigma^2}{2\sigma_t^2})^{N_r}\frac{1}{\prod_{i=1}^{N_r}\nu_{ri}^2}\sum_{j=1}^{N_r}(\prod_{k=1,k\neq j}^{N_r}\frac{1}{\mu_k-\mu_j}) \\ &\quad\times\int_0^\infty\frac{e^{-\mu_j s}}{s-2\mu}ds)^+ \end{aligned} \tag{58}$$

where the last integral is not an analytic integral and can be expressed in terms of an exponential integral. From (58) it can be inferred that more power should be assigned to a transmitter having lower $\prod_{i=1}^{N_r}\nu_{ri}^2$, which corresponds to having higher $\prod_{i=1}^{N_r}(r_{1i}r_{2i})^2$. In other words, in order to compensate the effect of pathloss, more power should be assigned at higher bistatic ranges. Consequently, we calculate the P_i and change parameter μ to hold the whole power equal to P. If P_i for some i's is negative, we put their power equal to zero and recalculate the other P_i values.

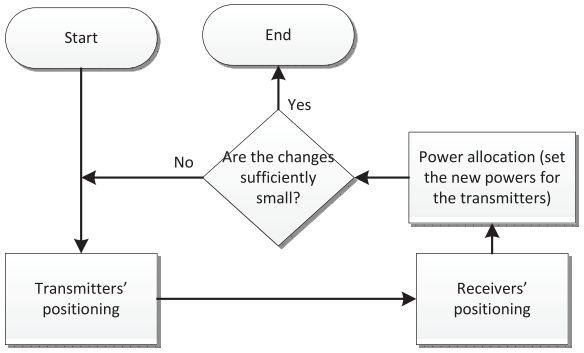

Fig. 1. Block diagram of algorithm.

V. IMPROVING THE ALGORITHM THROUGH SUCCESSIVE OPTIMIZATIONS

In Sections II and III, transmit and receive antennas' positions were determined assuming that all transmitters have the same power. Using the resulting positions, we proposed a power allocation scheme in Section IV in order to improve the detection performance. At this stage, we can further improve performance, by using the allocated powers as the powers used in the antennas' positioning. In other words, we repeat transmit and receive antennas' positioning using the new power levels, iteratively. Next, the power allocation is repeated using the new antennas' positions. This procedure of improving the results of antennas' positions using the allocated powers will be repeated until a satisfying convergence is obtained. The block diagram of the overall algorithm is shown in Fig. 1.

VI. SIMULATIONS

In our simulations, we assume a square-shaped region with sides equal to 30 km. The goal is to place three transmitters and three receivers in a widely separated MIMO configuration. In addition, the powers transmitted should be determined such that the total power is 30 kW.

Also, in order to obtain a more practical scenario, we use a priority function that defines the value of importance of each location from the detection point of view, with a value ranging from 0 to 1. In other words, the places with a higher degree of importance are assigned higher values in the priority function so that detecting the object in those places is more emphasized. By use of such criteria, the procedure of placing the transmitters and receivers differs a little from the one described before. The difference is that the reciprocal of this priority function's value at each location is also multiplied by the weighting coefficient. In this way, the value of the criterion used in the process of placing transmit and receive antennas is prioritized where the priority function has higher values. The priority function used in the simulations is shown in Fig. 2. It is inferred that the two points at (3.15, -7.35) km, (-8.45, 3.55) km have the highest priorities.

Subsequently, we apply the process described in Section II to choose the positions of the three transmit antennas. The result is shown in Fig. 3. The power gained at each location from the three positioned transmitters is also shown.

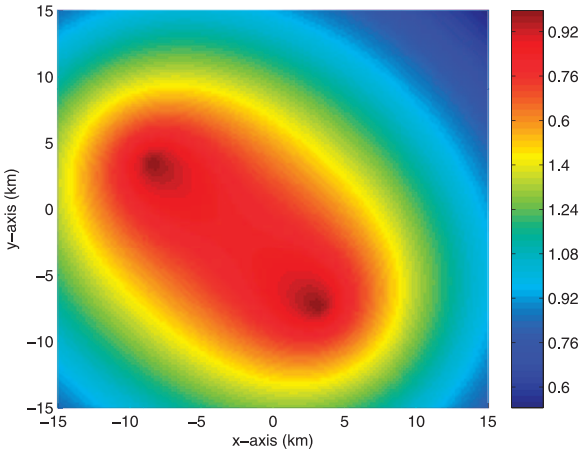

Fig. 2. Priority function.

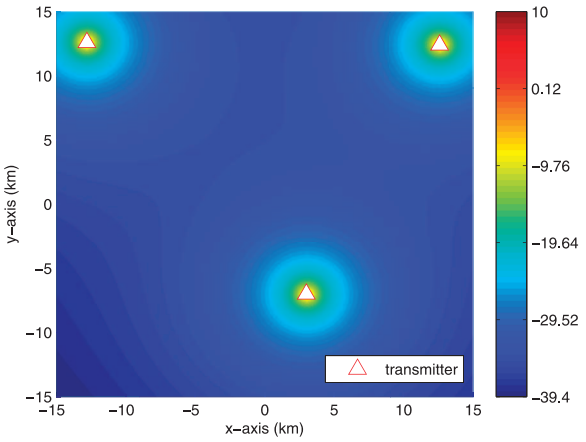

Fig. 3. Power gained at each point from three positioned transmitters.

TABLE II
Receive Antennas Positions

Receiver	x(km)	y(km)
#1	-1.4	-1.4
#2	-10.4	-8.8
#3	10.4	-4.2

Now, we locate the positions of the three receivers based on the procedure described in Section III using the priority function mentioned earlier. As described there, the positions are chosen one by one, using the SNR obtained from the previously positioned receiver(s) as the weighting coefficients. The result of receivers' positions obtained using this procedure is shown in Table II.

Finally, using the waterfilling power allocation scheme proposed in Section IV, the powers dedicated to the transmitters are listed in Table III. It can be verified that the power assigned to transmitter 1 is lower than the others. In fact, due to its vicinity to the receivers, the overall bistatic ranges resulting from this transmitter are lower, which as described earlier, leads to lower dedicated power level.

TABLE III
Powers Allocated to Transmitters after Waterfilling

Transmitter	x(km)	y(km)	power(kW)
#1	3.0	-7.0	5.748
#2	-12.8	12.6	12.659
#3	12.6	12.4	11.593

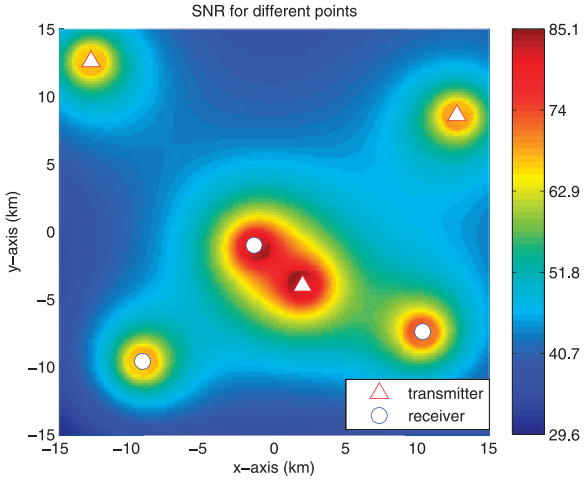

Fig. 4. Antennas' geometry and overall SNR after fourth iteration.

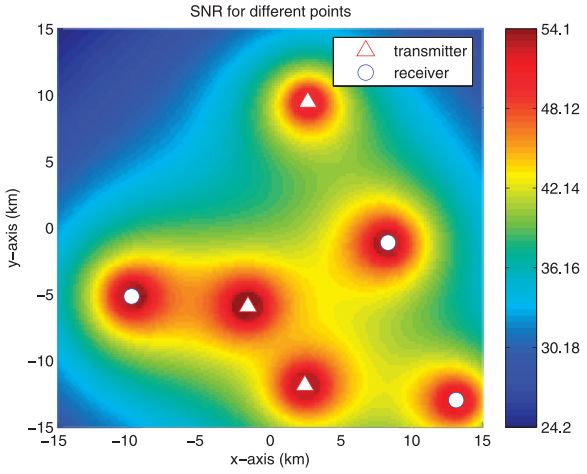

Fig. 5. Overall SNR for arbitrary antenna geometry with equal transmit powers.

In order to achieve a more efficient procedure, we can repeat the previous steps as described in Section V. For the scenario of our interest, a satisfying convergence can be achieved after three more iterations. The resulting powers for the three transmitters of Table III are 5.777 kW, 13.557 kW, and 10.666 kW, respectively. Also the antennas' geometry and SNR plot, after the fourth iteration, are shown in Fig. 4.

In order to show the power allocation and geometry's influence on the detection performance, the overall SNR for an arbitrary antenna positioning with the transmitters having the same power (each 10 kW) is shown in Fig. 5. Comparing this result with Fig. 4, the dependence of the detection on the antennas' positions and the powers allocated is observed. Also the average weighted receiver operating characteristic (ROC) (ROC averaged over the whole region, changing the target's position and weighted with the priority function) for these two cases are depicted in Fig. 6, which verifies the improvement of the proposed procedure.

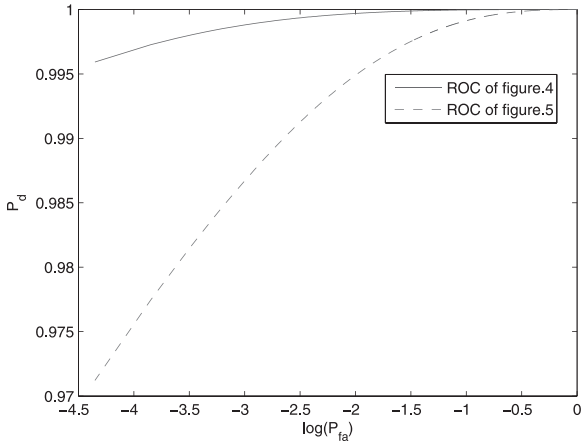

Fig. 6. Average weighted ROC.

VII. CONCLUSION

After designing the Neyman-Pearson detector for a Rayleigh scatter model in a MIMO configuration, we showed that the detection performance critically depends on the geometry of transmit and receive antennas. As the resulting power and SNR are highly dependent on the relative positions of transmitters, receivers, and the object to be localized, it can be a good criterion for choosing the positions of the antennas. Accordingly, we proposed a procedure to place transmit antennas and then receive antennas. It should be noted that the optimal solution is to place all antennas simultaneously according to the proposed criteria, but because of high complexity we developed a suboptimal procedure to locate the antennas one after another. Subsequently, we addressed the problem of assigning the transmitters' powers under the total power constraint. With this goal in mind, using the results of the designed detector, we arrived at a waterfilling-type method used in traditional MIMO wireless communication system designs.

APPENDIX A. SUM OF INDEPENDENT EXPONENTIALS

LEMMA 1. *Let* $(X_i)_{i=1\ldots n}$, $n \geq 2$, *be independent exponential random variables with pairwise distinct respective parameters* λ_i. *Then, the density of their sum is*

$$f_{X_1+X_2+\ldots+X_n}(x) = \left[\prod_{i=1}^{n}\lambda_i\right]\sum_{j=1}^{n}\frac{e^{-\lambda_j x}}{\prod_{\substack{k\neq j\\k=1}}^{n}(\lambda_k-\lambda_j)}, \quad x>0. \tag{59}$$

PROOF. First, we compute the convolutions required in the proof.

$$\begin{aligned} \mathrm{e}^{-ax} * \mathrm{e}^{-bx} &= \int_0^x \mathrm{e}^{-a(x-u)}\, \mathrm{e}^{-bu} \mathrm{d}u \\ &= \mathrm{e}^{-ax} \frac{\mathrm{e}^{(a-b)x} - 1}{a-b} = \frac{\mathrm{e}^{-bx} - \mathrm{e}^{-ax}}{a-b}. \end{aligned} \tag{60}$$

For $n = 2$,

$$\begin{aligned} f_{X_1+X_2}(x) &= f_{X_1}(x) * f_{X_2}(x) \\ &= \lambda_1\lambda_2 \frac{\mathrm{e}^{-\lambda_2 x} - \mathrm{e}^{-\lambda_1 x}}{\lambda_1 - \lambda_2} \\ &= \lambda_1\lambda_2 \left[\frac{\mathrm{e}^{-\lambda_1 x}}{\lambda_2 - \lambda_1} + \frac{\mathrm{e}^{-\lambda_2 x}}{\lambda_1 - \lambda_2} \right], \end{aligned} \tag{61}$$

in accordance to (59). Now, inductively, we fix $n \geq 3$, and assume the statement is true for $n-1$. Then

$$\begin{aligned} f_{X_1+X_2+\ldots+X_n}(x) &= f_{X_1+X_2+\ldots+X_{n-1}}(x) * f_{X_n}(x) \\ &= \left[\prod_{i=1}^{n-1} \lambda_i \right] \sum_{j=1}^{n-1} \frac{\mathrm{e}^{-\lambda_j x}}{\prod\limits_{\substack{k\neq j \\ k=1}}^{n-1} (\lambda_k - \lambda_j)} * f_{X_n}(x) \\ &= \left[\prod_{i=1}^{n} \lambda_i \right] \sum_{j=1}^{n-1} \frac{\mathrm{e}^{-\lambda_n x} - \mathrm{e}^{-\lambda_j x}}{(\lambda_j - \lambda_n) \prod\limits_{\substack{k\neq j \\ k=1}}^{n-1} (\lambda_k - \lambda_j)} \\ &= \left[\prod_{i=1}^{n} \lambda_i \right] \left[\sum_{j=1}^{n-1} \frac{\mathrm{e}^{-\lambda_j x}}{\prod\limits_{\substack{k\neq j \\ k=1}}^{n} (\lambda_k - \lambda_j)} - \sum_{j=1}^{n-1} \frac{\mathrm{e}^{-\lambda_n x}}{\prod\limits_{\substack{k\neq j \\ k=1}}^{n} (\lambda_k - \lambda_j)} \right] \end{aligned}$$

The proof is done as we show that the coefficient of $\mathrm{e}^{-\lambda_n x}$ fits the coefficients seen in the sum of (59), i.e.,

$$-\sum_{j=1}^{n-1} \frac{1}{\prod\limits_{\substack{k\neq j \\ k=1}}^{n} (\lambda_k - \lambda_j)} = \frac{1}{\prod\limits_{k=1}^{n-1} (\lambda_k - \lambda_n)} \tag{62}$$

or, equivalently,

$$\sum_{j=1}^{n} \frac{1}{\prod\limits_{\substack{k\neq j \\ k=1}}^{n} (\lambda_k - \lambda_j)} = 0.$$

Subsequently, we will have

$$\sum_{j=1}^{n} \frac{1}{\prod\limits_{\substack{k\neq j \\ k=1}}^{n} (\lambda_k - \lambda_j)} = \sum_{j=1}^{n} \frac{\prod\limits_{\substack{k\neq l\neq j \\ k,l=1}}^{n} (\lambda_k - \lambda_l)}{\prod\limits_{\substack{k\neq j \\ k,l=1}}^{n} (\lambda_k - \lambda_l)}$$

which is zero, if and only if

$$\sum_{j=1}^{n} \prod_{\substack{k\neq l\neq j \\ k,l=1}}^{n} (\lambda_k - \lambda_l)$$

is zero. We transform the latter in the following display.

$$\begin{aligned} &\sum_{j=1}^{n} \prod_{\substack{k\neq l\neq j \\ k,l=1}}^{n} (\lambda_k - \lambda_l) \\ &= \sum_{j=1}^{n} \prod_{\substack{j\neq k\neq l\neq j \\ k,l=1}}^{n} (\lambda_k - \lambda_l) \prod_{\substack{k=j\neq l \\ k,l=1}}^{n} (\lambda_k - \lambda_l) \\ &= \pm \sum_{j=1}^{n} \prod_{\substack{j\neq k>l\neq j \\ k,l=1}}^{n} (\lambda_k - \lambda_l)^2 \prod_{\substack{k=j>l \\ k,l=1}}^{n} (\lambda_k - \lambda_l) \prod_{\substack{k=j<l \\ k,l=1}}^{n} (\lambda_k - \lambda_l) \\ &= \pm \sum_{j=1}^{n} \prod_{\substack{j\neq k>l\neq j \\ k,l=1}}^{n} (\lambda_k - \lambda_l)^2 \prod_{\substack{j=k>l \\ k,l=1}}^{n} (\lambda_k - \lambda_l) \prod_{\substack{k>l=j \\ k,l=1}}^{n} (\lambda_k - \lambda_l)(-1)^{n-j} \\ &= \pm \prod_{\substack{k>l \\ k,l=1}}^{n} (\lambda_k - \lambda_l) \sum_{j=1}^{n} \prod_{\substack{j\neq k>l\neq j \\ k,l=1}}^{n} (\lambda_k - \lambda_l)(-1)^{n-j}, \end{aligned} \tag{63}$$

which is zero, if and only if

$$\sum_{j=1}^{n} \prod_{\substack{j\neq k>l\neq j \\ k,l=1}}^{n} (\lambda_k - \lambda_l)(-1)^j \tag{64}$$

is zero. Notice that the product is a Vandermonde determinant of the form

$$\begin{vmatrix} 1 & \lambda_1 & \lambda_1^2 & \cdots & \lambda_1^{n-2} \\ 1 & \lambda_2 & \lambda_2^2 & \cdots & \lambda_2^{n-2} \\ \vdots & \vdots & \vdots & \ddots & \vdots \\ 1 & \lambda_{j-1} & \lambda_{j-1}^2 & \cdots & \lambda_{j-1}^{n-2} \\ 1 & \lambda_{j+1} & \lambda_{j+1}^2 & \cdots & \lambda_{j+1}^{n-2} \\ \vdots & \vdots & \vdots & \ddots & \vdots \\ 1 & \lambda_n & \lambda_n^2 & \cdots & \lambda_n^{n-2} \end{vmatrix},$$

and hence, (64) is equal to the expansion of the determinant

$$\begin{vmatrix} 1 & 1 & \lambda_1 & \lambda_1^2 & \cdots & \lambda_1^{n-2} \\ 1 & 1 & \lambda_2 & \lambda_2^2 & \cdots & \lambda_2^{n-2} \\ \vdots & \vdots & \vdots & \vdots & \ddots & \vdots \\ 1 & 1 & \lambda_n & \lambda_n^2 & \cdots & \lambda_n^{n-2} \end{vmatrix}$$

w.r.t. its second column. As this determinant is zero, so is (64) and thus, (62) is proved.

APPENDIX B. T IS A MONOTONICALLY INCREASING FUNCTION OF $\frac{a_{2ri}}{a_{1ri}}$

For certain i and r, the test statistic (T), defined in (33), is a function of $\frac{a_{2ri}}{a_{1ri}}$ as below

$$\mathrm{Log}(1+\frac{a_{2ri}}{a_{1ri}}\sqrt{\pi}e^{\frac{a_{2ri}^2}{4a_{1ri}^2}}Q(-\frac{a_{2ri}}{\sqrt{2}a_{1ri}})) \tag{65}$$

The argument of the logarithm function is the product of three functions:

$$f_1(\frac{a_{2ri}}{a_{1ri}})=\frac{a_{2ri}}{a_{1ri}} \tag{66}$$

$$f_2(\frac{a_{2ri}}{a_{1ri}})=e^{\frac{a_{2ri}^2}{4a_{1ri}^2}} \tag{67}$$

$$f_3(\frac{a_{2ri}}{a_{1ri}})=Q(-\frac{a_{2ri}}{\sqrt{(2)}a_{1ri}}) \tag{68}$$

which are all monotonically increasing functions of their arguments, and therefore, $\frac{a_{2ri}}{a_{1ri}}$. Consequently, the product of these three functions is monotonically increasing as well. As a result, the statistic is a monotonically increasing function of $\frac{a_{2ri}}{a_{1ri}}$.

REFERENCES

[1] Haimovich, A. M., Blum, R. S., and Cimini, L. J.
MIMO radar with widely separated antenna.
IEEE Signal Processing Magazine, **25**, 1 (2007), 116–129.

[2] Li, J., and Stoica, P.
MIMO radar with colocated antennas.
IEEE Signal Processing Magazine, **24**, 5 (2007), 106–114.

[3] Radmard, M., Karbasi, S. M., Khalaj, B. H., and Nayebi, M. M.
Data association in multi-input single-output passive coherent location schemes.
IET Radar, Sonar & Navigation, **6**, 3 (2012), 149–156.

[4] Radmard, M., Karbasi, S. M., and Nayebi, M. M.
Data Fusion in MIMO DVB-T-based passive coherent location.
IEEE Transactions on Aerospace and Electronic Systems, **49**, 3 (July 2013), 1725–1737.

[5] Lehmann, N. H., Fishler, E., Haimovich, A. M., Blum, R. S., Chizhik, D., Cimini, L. J., and Valenzuela, R. A.
Evaluation of transmit diversity in MIMO-radar direction finding.
IEEE Transactions on Signal Processing, **55**, 5 (2007), 2215–2225.

[6] Fishler, E., Haimovich, A., Blum, R. S., Cimini, L. J., Chizhik, D., and Valenzuela, R. A.
Spatial diversity in radars-models and detection performance.
IEEE Transactions on Signal Processing, **54**, 3 (2006), 823–838.

[7] Fishler, E., Haimovich, A., Blum, R., Chizhik, D., Cimini, L., and Valenzuela, R.
MIMO radar: An idea whose time has come.
In *Proceedings of the IEEE Radar Conference*, 2004, pp. 71–78.

[8] Godrich, H., Haimovich, A. M., and Blum, R. S.
Cramer Rao bound on target localization estimation in MIMO radar systems.
In *42nd Annual Conference on Information Sciences and Systems*, 2008, pp. 134–139.

[9] Godrich, H., Haimovich, A. M., and Blum, R. S.
Target localization accuracy gain in MIMO radar-based systems.
IEEE Transactions on Information Theory, **56**, 6 (2010), 2783–2803.

[10] Godrich, H., Haimovich, A. M., and Blum, R. S.
Target localisation techniques and tools for multiple-input multiple-output radar.
IET Radar, Sonar & Navigation, **3**, 4 (2009), 314–327.

[11] He, Q., Blum, R. S., Godrich, H., and Haimovich, A. M.
Target velocity estimation and antenna placement for MIMO radar with widely separated antennas.
IEEE Journal of Selected Topics in Signal Processing, **4**, 1 (2010), 79–100.

[12] Radmard, M., Khalaj, B. H., Chitgarha, M. M., Nazari-Majd, M., and Nayebi, M. M.
Receivers' positioning in MIMO DVB-T based passive coherent location.
IET Radar, Sonar & Navigation, **6**, 7 (2012), 603–610.

[13] Nazari-Majd, M., Chitgarha, M. M., Radmard, M., and Nayebi, M. M.
Probability of missed detection as a criterion for receiver placement in MIMO PCL.
In *IEEE Radar Conference* (RADAR), 2012, pp. 924–927.

[14] Chitgarha, M. M., Nazari-Majd, M., Radmard, M., and Nayebi, M. M.
Choosing the position of the receiver in a MISO passive radar system.
In *9th European Radar Conference* (EuRAD), 2012, pp. 318–321.

[15] Akhtar, J.
Energy allocation for correlated MIMO radar antennas with Ricean targets.
In *11th International Radar Symposium* (IRS), 2010, pp. 1–4.

[16] Akcakaya, M., and Nehorai, A.
MIMO radar detection and adaptive design in compound-Gaussian clutter.
In *IEEE Radar Conference*, 2010, pp. 236–241.

[17] Akcakaya, M., and Nehorai, A.
Adaptive MIMO radar design and detection in compound-Gaussian clutter.
IEEE Transactions on Aerospace and Electronic Systems, **47**, 3 (2011), 2200–2207.

[18] Gogineni, S. and Nehorai, A.
Target estimation using sparse modeling for distributed MIMO radar.
IEEE Transactions on Signal Processing, **59**, 11 (2011), 5315–5325.

[19] Aittomaki, T., Godrich, H., Poor, H. V., and Koivunen, V.
Resource allocation for target detection in distributed MIMO radars.
In *Forty Fifth Asilomar Conference on Signals, Systems and Computers* (ASILOMAR), 2011, pp. 873–877.

[20] Godrich, H., Petropulu, A., and Poor, H. V.
Resource allocation schemes for target localization in distributed multiple radar architectures.
In *Proceedings of European Signal Processing Conference*, 2010.

[21] Poor, H. V.
An Introduction to Signal Detection and Estimation. New York: Springer, 1994.

M. Radmard received the B.S., M.S., and Ph.D. degrees in electrical engineering, all from Sharif University of Technology, Tehran, Iran.

He is now working as a postdoc researcher at the same university. His research interests include MIMO systems, passive coherent location, signal processing, and speech processing.

M. M. Chitgarha (S'12) received his B.Sc and M.Sc. degrees in the communications field from Sharif University of Technology, Tehran, Iran. He was ranked first in both M.Sc. and Ph.D. national university entrance exams. He is now a Ph.D. candidate at the same university.

His research interests include MIMO radars, radar signal processing, detection theory, and speech signal processing.

M. Nazari-Majd (S'12) received B.Sc.Eng and M.Sc.Eng degrees in the communications field from Sharif University Technology, Tehran, Iran. He was approved as top talent in both B.Sc. and M.Sc. from the university. He is currently working toward his Ph.D. degree at the same university.

His research interests include MIMO radars, noise radars, detection theory, and radar signal processing.

He was a member of the Iranian Physics' Olympiad team in 2008.

M. M. Nayebi (S'89—M'94—SM'05) received the B.S. and M.S. degrees from Sharif University of Technology, Tehan, Iran, and the Ph.D. degree in electrical engineering, from Tarbiat Modarres University, Tehran, Iran.

He joined the Sharif University of Technology faculty in 1994. His main research interests are radar signal processing and detection theory.